A Novel Radar-Magnetic Technique for Dielectric Permittivity Mapping of Bridge Decks in Order to Determine Moisture and Salinity of the Concrete

Hans-Joachim KRAUSE, Thorsten WINKLER, Coralie DANG, Daniel OWSIEJEWICZ, Forschungszentrum Jülich, Germany
Gottfried SAWADE, Materialprüfungsanstalt (MPA) Otto-Graf-Institut, University of Stuttgart, Germany
Frank DUMAT, Baustoff- und Bodenprüfstelle Kassel, Germany
Edmund RATH, Bundesanstalt für Straßenwesen, Bergisch Gladbach, Germany

Abstract. For the assessment of the condition of concrete bridge decks it is important to know the moisture and the salinity of the concrete. Usually, the salinity is determined by potential measurements and is verified by analyzing samples in the laboratory. However, this method requires the removal of the pavement. We developed a novel technique for nondestructive determination of the complex dielectric permittivity of the concrete which operates nondestructively from a wagon running on the pavement. Using a 1 GHz Ground Penetrating Radar, the transient time of the electromagnetic wave to the upper layer reinforcement bars (rebars) is measured. The depth of the rebars is determined by a magnetic measurement of two components of the static magnetic field of the premagnetized rebars using feedback-linearized GMR magnetometers. This magnetic depth determination technique is independent of the dielectric properties of the materials covering the rebars. Comparison of the Radar delay and the magnetically extracted depth yields the averaged real part of the dielectric permittivity of the intermediate material. The imaginary part of the dielectric permittivity is estimated from the reflected Radar amplitude. The moisture and salt content of the concrete is derived from the measured complex dielectric permittivity using interpolated calibration curves. The method was evaluated using a test block of reinforced concrete with water and chloride contaminated nests and an asphalt cover slab, resembling a typical bridge deck. The system was tested on two highway bridge decks. The dielectric constant of the concrete close to the surface was mapped. The advantages and the limitations of the new technique are discussed.

1. Introduction

The increasing load on highway bridges due to increasing heavy goods vehicle traffic, aging and problems with the durability of structures may lead to obstructions of traffic with ensuing severe economic damages. In Germany, bridges and other concrete structures are regularly inspected. However, the inspections are mainly carried out visually. Therefore,

damages are only identified when the deterioration becomes visible. There is ample demand for test methods to establish the condition of structures as early as possible. Non-destructive test methods may provide a cost-effective means to establish whether a structure is still in a serviceable condition or not [1]. Thus, effective planning of repair measures becomes feasible, allowing to minimize service costs and safely avoiding heavy damages.

Most of the concrete highway bridges in Germany are prestressed in both longitudinal and transverse directions. The bridge deck is covered with a sealing layer and a bituminous layer serving as a protection barrier against water infiltration. However, most of the sealing layers from the 1960's and 1970's have deteriorated in the meantime, permitting salt-contaminated water to seep into the concrete. It is hardly possible to detect these sites visually. Therefore, methods to localize moist and chloride-contaminated areas in the concrete are particularly important. State of the art in non-destructive evaluation of moisture and salinity are potential measurement and electromagnetic techniques [2]. The potential method is based on recording the difference in electric potential on the concrete surface against an electrical contact of the reinforcement by means of wetted conducting wheels [3]. Measurement systems with a number of wheels in parallel are available which allow to scan large areas the concrete surface. This technique, however, is only applicable on the bridge deck after milling off the asphalt pavement and the sealing layer. In the GHz frequency range, it is in principle possible to independently determine moisture and salinity [4,5]. However, the microwave techniques are either limited to surface regions or require two-sided access or boreholes. The most reliable determination of the chloride content relies on drilling out samples and performing a chemical analysis in the laboratory [6].

The goal of our work is the development of a technique that allows to determine independently the moisture and salinity of concrete structures, even through a covering pavement layer.

Our novel technique is based on the following idea: bridge decks contain a rather dense layer of steel reinforcement bars (rebars) at shallow depths of a few cm. These rebars act as reflectors of Radar pulses. The measurement of the transient time of a 1 GHz Radar pulse to a rebar and back yields the propagating velocity of the electromagnetic wave if the depth of the bar is known. From the velocity and from the amplitude of the reflected pulse, the complex dielectric permittivity can be deduced. From the dielectric properties at a frequency of 1 GHz, the moisture and the salinity of the intermediate material may be derived independently [4]. However, we do need to know the precise depth of each rebar.

For the determination of the depth of steel rebars or the thickness of the concrete cover, two electromagnetic techniques are used in practice [2,7]: the eddy current technique and the static magnetic technique. Both methods usually require knowledge of the diameter of the steel reinforcement bars. For the eddy current technique, an approach utilizing phase analysis for the suppression of the effect of the steel diameter on the signal has been reported [8]. In practice, numerous disturbing effects such as crossings, edges or densely packed reinforcement may occur. In addition, material parameters of the steel, the electrical AC conductivity of the concrete and even the speed of the measurement vehicle may have detrimental effects on the accuracy of the eddy current measurement. In contrast, the static magnetic stray flux technique is barely influenced by these effects. However, variations in the magnetic permeability of the steel bars does significantly impair the precision [9].

Our technique is a refinement of the static magnetic technique. It relies on a measurement of the remanent static magnetic field of the rebars after they have been premagnetized. From an appropriate combination of at least two of these field components, the depth of the steel bars can be calculated, see section 2.2. The quasi-static magnetic measurement is completely independent of the dielectric permittivity of the embedding concrete, whereas the velocity of the Radar wave is dependent on the real part of the dielectric constant. Comparison of the two allows to estimate salinity and moisture of the concrete.

2. Radar-Magnetic measurement technique

2.1. Radar reflection measurement

The Ground Penetrating Radar (GPR) method is based on sending radio frequency electromagnetic pulses into the medium and measuring the reflected signal as a function of the delay time *t* [10]. Fig. 1 depicts schematically the Radar reflection at the interfaces.

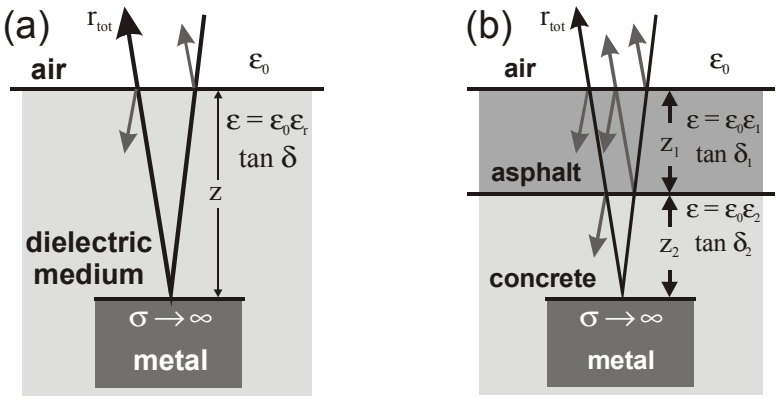

Fig. 1. (a) Schematic of the Radar reflection at a metal object (steel rebar) embedded in a dielectric medium (concrete). (b) Schematic of the Radar reflection for the case of an additional asphalt cover layer above the concrete. Additional refraction and multiple reflections have to be taken into account.

Solutions of the wave equation for the phasor vector derived from the source-free, instantaneous Maxwell equations are damped planar waves of the form

$$\mathbf{E}(z,\omega) = E_0 \exp(-\alpha z)\exp(-i\beta z) \tag{1}$$

(similarly for **H**) with the damping constant α and the phase constant β. In the case of a homogeneous, dielectric, nonmagnetic medium with losses that are not too large, i.e. a loss tangent $\tan\delta = \dfrac{\sigma}{\omega\varepsilon} = \dfrac{\varepsilon''}{\varepsilon_r} << 1$, the damping constant α and the phase constant β may be may be written and expanded for first order loss corrections as

$$\alpha = \frac{\omega}{c}\sqrt{\frac{\varepsilon_r}{2}\left[\sqrt{1+\tan^2\delta}-1\right]} \approx \frac{\omega}{c}\frac{\sqrt{\varepsilon_r}}{2}\tan\delta \tag{2}$$

$$\beta = \frac{\omega}{c}\sqrt{\frac{\varepsilon_r}{2}\left[\sqrt{1+\tan^2\delta}+1\right]} \approx \frac{\omega}{c}\sqrt{\varepsilon_r}\left(1+\frac{1}{8}\tan^2\delta\right) \tag{3}$$

Here, *c* denotes the vacuum velocity of light, $\omega = 2\pi f$ is the angular frequency of the wave, $\varepsilon = \varepsilon_0\varepsilon_r$ and $\mu = \mu_0$ are the dielectric and magnetic permittivities of the medium in which the reflector is embedded. The transmission coefficient for the orthogonal entry of a planar electromagnetic wave from a medium 1 into a medium 2 is given by $\tau = \dfrac{2\eta_2}{\eta_1+\eta_2}$

with the intrinsic impedance $\eta = \frac{E_0 \exp(-\alpha z)\exp(-i\beta z)}{H_0 \exp(-\alpha z)\exp(-i\beta z)} = \sqrt{\frac{i\omega\mu}{\sigma + i\omega\varepsilon}}$ of the waves in the respective medium given by the ratio of the phasors **E** and **H**.

In order to calculate the damping of the reflected Radar amplitude from a rebar, we assume the idealized case of a plane wave. We consider the refraction at the entry from air into the dielectric medium *m* (dielectric permittivity $\varepsilon = \varepsilon_0 \varepsilon_r$, dielectric losses tan δ), the passage through the medium, its reflection at a metal object, the passage back and the exit refraction back into air. The overall reflection coefficient r_{tot} consists of both transmission coefficients (air-medium and medium-air) and twice the damping inside the medium, which may be written and expanded for small losses as follows:

$$r_{tot} = \frac{2\eta_m}{\eta_m + \eta_0} \exp(-2\alpha z) \frac{2\eta_0}{\eta_m + \eta_0} \approx \frac{\frac{4}{\sqrt{\varepsilon_r}}}{\left[\frac{1}{\sqrt{\varepsilon_r}} + 1\right]^2} \exp\left(-\frac{\omega z}{c}\sqrt{\varepsilon_r}\tan\delta\right) \tag{4}$$

The complex dielectric permittivity of the medium can be extracted by inversion of Eq. (3) for the wave velocity and by using the simplified Eq. (4) for the reflection coefficient from the measured quantities transient time t_r and amplitude $A_r = r_{tot} A_0$ of the Radar echo of a steel rebar at a depth *z*. One obtains in first order approximation:

$$\sqrt{\varepsilon_r} \approx \frac{ct_r}{2\sqrt{(x - x_B)^2 + z^2}}\left(1 - \frac{1}{8}\tan^2\delta\right) \xrightarrow[\tan\delta \to 0]{x \to x_B} \frac{ct_r}{2z} \tag{5}$$

$$\tan\delta \approx \frac{c}{\omega z\sqrt{\varepsilon_r}} \ln\left[\frac{\left(\frac{1}{\sqrt{\varepsilon_r}} + 1\right)^2 r_{tot}}{\frac{4}{\sqrt{\varepsilon_r}}}\right] \tag{6}$$

Here, x_B and *z* denote the lateral and vertical position of the reflector. If the depth *z* of a reflector is known (e.g. from the magnetic measurement, Section 2.2) and the losses are completely neglected, Eq. (5) yields a first approximation of the dielectric permittivity ε_r of the medium. Inserting this ε_r into Eq. (6) leads to a first approximation of the losses tan δ. By iterative insertion of the first order tan δ from Eq. (6) into Eq. (5) and so forth, the precision of a solution pair ε_r and tan δ may easily be improved successively.

In the case of an additional asphalt layer (Fig. 1b), additional refraction and multiple reflections have to be taken into account. Additional terms and a second set of material parameters ε and tan δ of asphalt appear in Eqs. (5) and (6). In case these values are known by other means, these expanded formulas should be used. Our calculations, however, were performed using Eqs. (5) and (6).

2.2. Static magnetic depth determination

In this contribution, an improvement of the static magnetic technique [9] is proposed which is based on recording several components of the magnetic gradient tensor. This technique

allows to determine the depth of the bars independent of their diameter, of their magnetization state and of their magnetic permeability. The magnetic depth determination method is based on a measurement of the remanent magnetic field after magnetization by means of a permanent magnet. The magnetization of a single steel reinforcement bar, oriented in y direction, is almost completely dominated by its y component, $M(y)$. Therefore, the scalar magnetic potential of that bar, at a vertical distance z from the scanning direction x and a lateral position x_B, may be written as:

$$\psi(x,z) = -\frac{1}{4\pi}\int \frac{A \cdot \frac{d}{dy'} M(y')\, dy'}{\sqrt{(x-x_B)^2 + y'^2 + z^2}} \tag{7}$$

Here, $M(y)$ denotes the position-dependent magnetization of the bar and A is a constant dependent on the unit system.

The magnetic field components are given by the derivative of the potential with respect to x: $H_x(x,z) = \frac{\partial}{\partial x}\Psi(x,z)$, and z: $H_z(x,z) = \frac{\partial}{\partial z}\Psi(x,z)$. From Eq. (7), it is easily seen that the following fundamental relation holds for the field components H_x und H_z, independent of the magnetization distribution $M(y)$ of the bar:

$$zH_x - (x - x_B)H_z = 0 \tag{8}$$

Eq. (8) may be considered as the fundamental equation of magnetic depth determination. By performing derivatives of (8) with respect to x und z and solving them for z, different equation for the depth of the rebar, z, may be derived. If (8) is differentiated once with respect to x, the following equation based on the quotient of one magnetic field component and one first order gradient is obtained:

$$z = \frac{H_z + (x - x_B)H_{x,z}}{H_{x,x}} \xrightarrow{x \to x_B} \frac{H_z}{H_{x,x}} \tag{9}$$

Solving the second order derivatives of (8) with respect to x and z for z leads to an equation which contains gradients of first and second order:

$$z = \frac{H_{z,z} - H_{x,x} + (x - x_B)H_{x,zz}}{H_{x,xz}} \xrightarrow{x \to x_B} \frac{H_{z,z} - H_{x,x}}{H_{x,xz}} \tag{10}$$

Similarly, the third derivative of (8) with respect to x may be written as the following non-singular expression for the depth z of the rebar:

$$z = \frac{3H_{z,xx} - (x - x_B)H_{z,xxx}}{H_{x,xxx}} \xrightarrow{x \to x_B} \frac{3H_{z,xx}}{H_{x,xxx}} \tag{11}$$

In principle, equations for the depth z containing derivatives of arbitrary order may be found. The higher the order, the less sensitive the equation should be against effects from neighbouring steels. However, the higher the order, the higher is the noise in the numerically evaluated derivative. In practice, when trying to determine which formula is best suited for the depth determination, one has to trade off noise against less influence from adjacent bars.

3. Setup of the measurement vehicle

We have set up a measurement system consisting of a ground penetrating radar, a magnet for generating a static magnetic field and a measurement head for recording the magnetic stray field. The system is configured for on-line inspection on board of a slow vehicle. Fig. 2 depicts schematically the principle of the measurement vehicle.

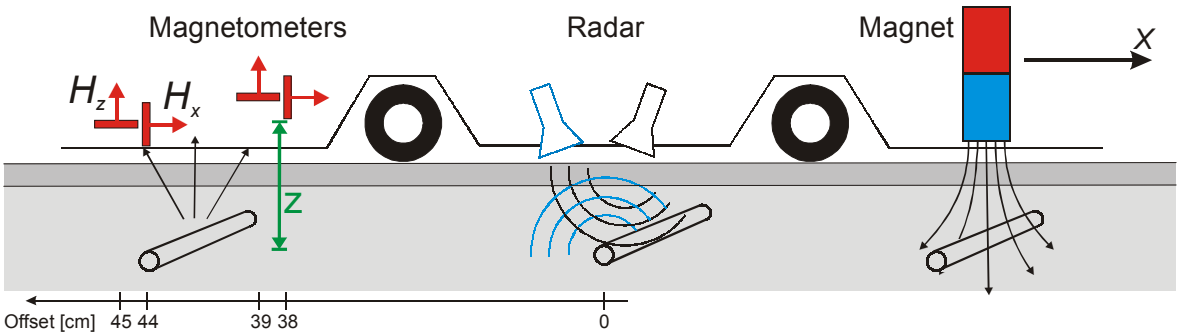

Fig. 2. Sketch of the measuring vehicle for determination of the dielectric permittivity and salinity of reinforced concrete by magnetic measurement of rebar position and depth and radar measurement of the reflection time. The vehicle carries a permanent magnet for magnetization of the steel reinforcement bars, a measurement head containing four GMR magnetometers and a 1 GHz Ground Penetrating Radar (GPR) head.

A measurement head containing four GMR magnetometer sensors (AA-002 of NVE, Inc.) was set up. Two magnetometers measure the component H_x, and two others the component H_z, each at two distinct, slightly different depth positions z, as sketched in Fig. 1. In order to achieve excellent linearity and temperature stability, the magnetometers are operated as null detectors in a constant field mode by feeding back the measured field by means of compensation coils [11]. The measurement head was mounted at the bottom rear side of the vehicle with 2 cm spacing to the ground. A strong permanent magnet for magnetizing the steel rebars in the concrete was affixed at the front, also about 2 cm above the ground. The Ground Penetrating Radar (RAMAC/GPR from MALÅ Geo-Science, with a bistatic 1 GHz sending and receiving antenna combination) was mounted in the middle of the vehicle with the same spacing. One of the four pneumatic tires was connected to a rotational quadrature encoder for recording the position of the vehicle. Every 0.063 mm, a position pulse triggers a magnetic measurement. A Radar impulse measurement is triggered every 9.4 mm. The measured Radar reflection signals of a line scan are depicted as a B-scan graph, resembling a depth profile along the scanning path.

4. Magnetic test measurements in the laboratory

Using the magnetometer sensor head, measurements of single mild steel reinforcement bars of 8 mm diameter were performed in the laboratory at different distances between bars and sensors. The measurements were conducted by mounting the bars perpendicular to the scanning path at different minimum distances z and scanning past the bars with a permanent magnet and subsequently with the magnetometer head. Fig. 3 shows the measured magnetic field components H_x (left) and H_z (right) as a function of the position x for different depths z ranging from 3 cm to 15 cm.

After numerical differentiation and filtering, the depth of the steel bar was calculated using Eqs. (9), (10) and (11). Fig. 4 shows the result. For short distances, all three formulas give precise results for the depth which agree well with the known real depth.

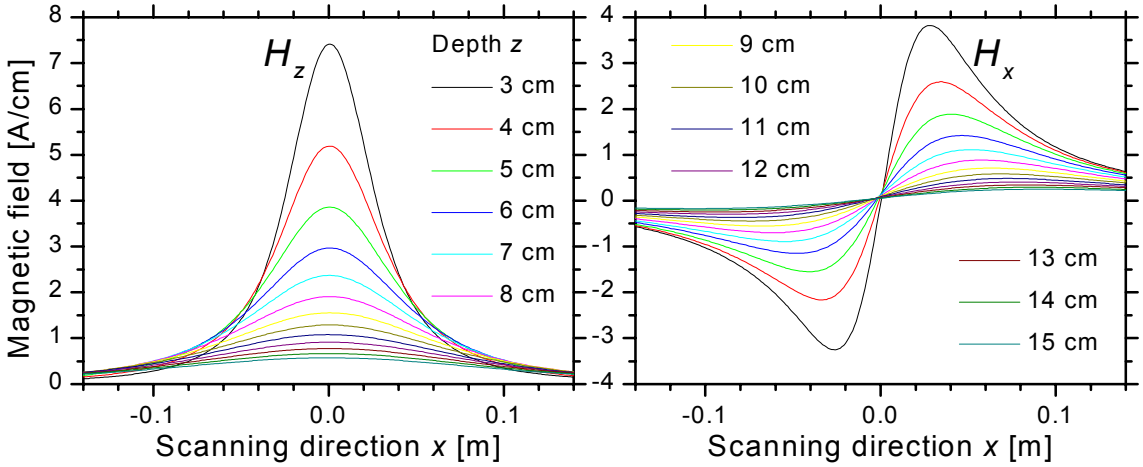

Fig. 3. Magnetic field component H_z (left) and H_x (right) as a function of the scan coordinate x for different distances (depths) z, measured during a laboratory scan across a steel bar at $x = 0$.

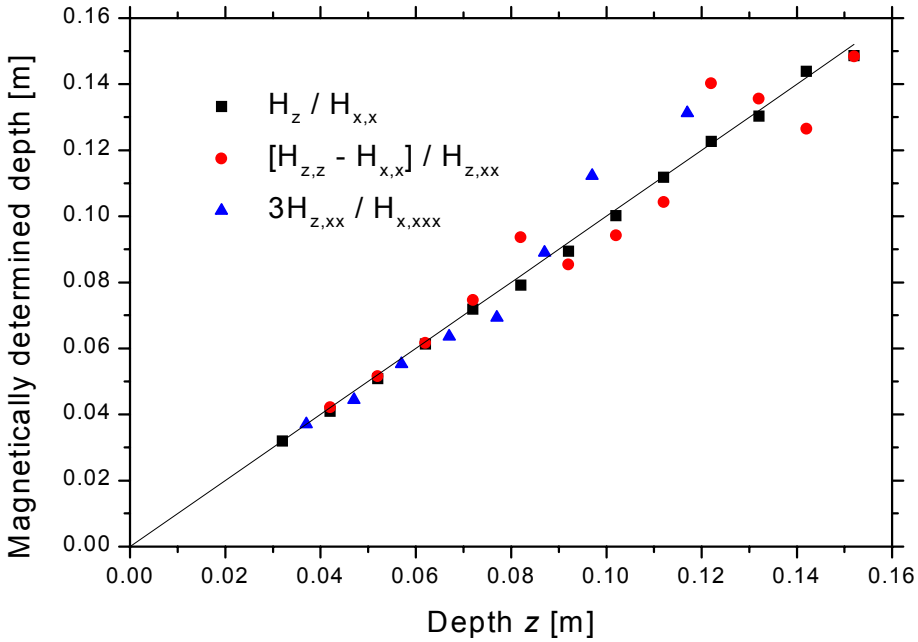

Fig. 4. Comparison of three different formulas for magnetic depth determination, based on magnetic field gradients of different orders. The magnetically determined depth is plotted against the real geometrical depth of the rebars.

For larger distances, deviations are observable especially in case of the higher order derivatives which are due to the increasing noise with higher order of numerical differentiation. Therefore, one could come to the conclusion that the formula with the lowest order possible, (9), would be the best one. This assumption, however, is wrong in case of a realistic situation at a building structure. In that case, the offset magnetic field is not known. Furthermore, one has to deal with the signals from neighbouring steel bars. This influence decreases with increasing order of differentiation. Therefore, one should use the highest differentiation order that still yields an acceptable signal-to-noise ratio in the derivative signals. In practice, this will depend strongly on the intrinsic noise of the magnetometer sensors and the environmental disturbance noise.

5. Measurements of concrete test blocks with chloride contaminations

A test block of reinforced concrete, designed to resemble a typical bridge deck, was manufactured for evaluation of the proposed method. The block with outer dimensions of 3 m × 1.4 m × 0.3 m was reinforced by steel bars of 12 mm diameter, arranged in a regular 20 cm × 20 cm grid at the top and the bottom of the block. The nominal depth of the upper rebar layer was 5 cm below the concrete surface, but turned out to be deeper in reality, see Fig. 3. At five locations on the upper surface of the block, chloride nests were introduced during manufacturing. Separated from the rest of the block by plastic tubing during concreting, five different concrete mixtures prepared with additional saline solution were prepared, forming 30 cm diameter pots of chloride-contaminated concrete.

With the magnetic sensor and the Radar, scans were performed along the long side of the test block. Fig. 5 (left) shows the measured magnetic field components H_x und H_z as a function of the scan coordinate x for the scan at y = 0.25 m. This scan runs across two of the prepared chloride nests, centered at x = 0.95 m and x = 2.15 m, respectively. By numerical differentiation and FIR filtering, the third order derivative of the tangential magnetic field with respect to the scanning direction x, the gradient component $H_{x,xxx}$, and the second derivative of the vertical field, the component $H_{z,xx}$ was calculated. Fig. 5 (right) displays the result.

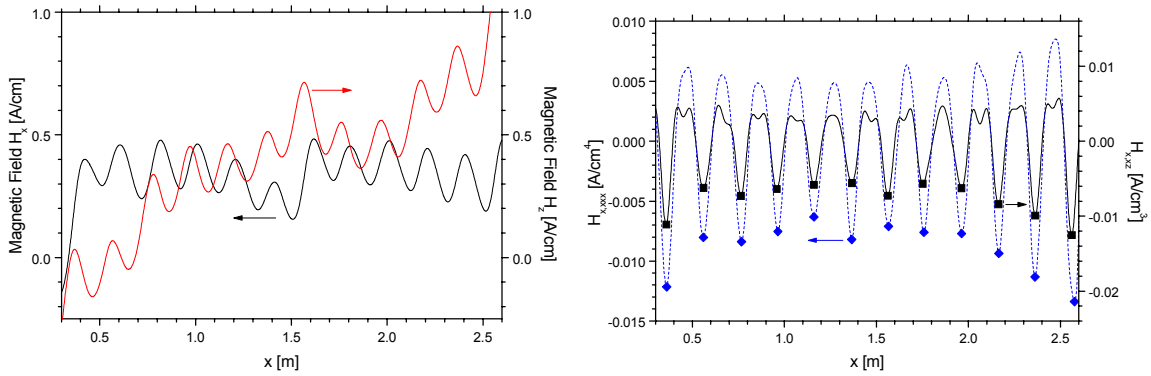

Fig. 5. Left: Magnetic field components H_x and H_z, measured on the test block. Right: Magnetic field gradients $H_{x,xxx}$ and $H_{z,xx}$, determined by numerically differentiating the measured components H_x and H_z three and two times with respect to x. The positions of the minima of the gradient components indicate the positions x_B of the rebars (full symbols).

The positions of the minima of the gradient components were selected as (magnetically) exact positions x_B of the rebars. Using Eq. (11), the depth was computed as the quotient of the two gradient components. The result is plotted as a solid line in Fig. 6. The black squares indicate the values at the rebar positions x_B which were taken as their respective (magnetic) rebar depths z. These values coincide reasonably well with the values determined by a commercial electromagnetic cover meter. At two positions, the exact depth was verified by opening the concrete.

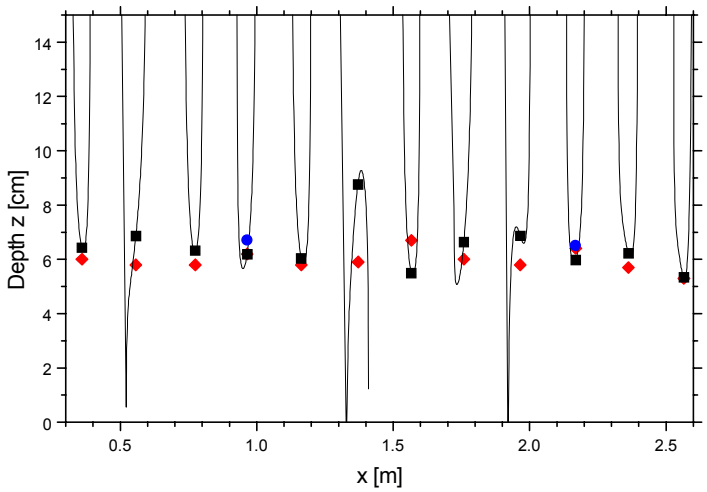

Fig. 6. Depth z of the rebars below the concrete surface, as calculated from the quotient of the magnetic field gradients $3H_{z,xx}$ and $H_{x,xxx}$, using Eq. (11). The black squares indicate the depth values at the respective rebar positions x_B. A spacing of 2.4 cm between magnetometers and concrete surface is taken into account. For comparison, the depth values measured with a commercial cover meter (Hilti Ferroscan) is given (red diamonds). At two positions, the depth was checked by opening the concrete (blue circles). Except for the values at x_B = 1.37 m and x_B = 1.57 m, the magnetically determined depth is in good agreement with the electromagnetic measurement.

Each steel bar running perpendicular to the scanning direction appears as a hyperbola in the Radar B-scan. Using a polynomial fit to the measured Radar data, the positions of the bars were determined from the apex positions of the hyperbolas. These positions were in good agreement with the bar positions extracted from the magnetic field measurements. By inserting the reflection time t from the Radar measurement and the rebar depth z from the magnetic measurement (Fig. 6) into Eq. (5), the effective dielectric permittivity ε_r was derived. Fig. 7 shows a surface plot of the ε_r values of the concrete block. In the vicinity of the rebars at x_B = 0.97 m and x_B = 2.17 m, the chloride content was determined by chemical analysis. Values of 0.6 and 0.8 mass % were found. The derived dielectric permittivity shows a systematic increase at three of the five chloride nests.

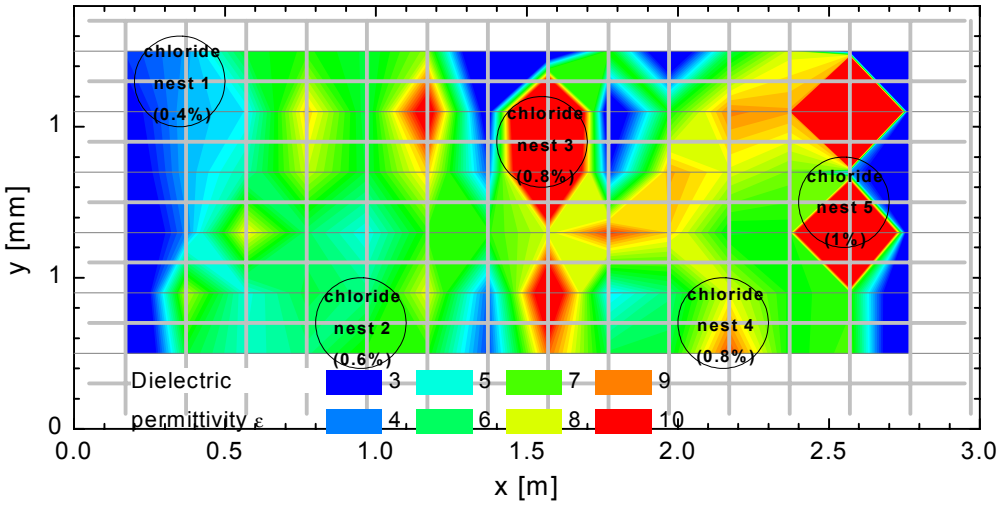

Fig. 7. Map of the real part of the effective dielectric permittivity ε of the concrete test block with chloride nests, as determined from the Radar transient time scans (thin gray lines) to the upper rebar layer (thick gray lines) and the magnetically determined depth.

In addition, Radar scans were performed using three cylindrical concrete samples (diameter 15 cm, height 10 cm). These samples were prepared with a porous concrete with a water/cement ratio w/z = 0.7. All three were vacuum-dried for two weeks and subse-

quently flooded with (salt-)water. The maximum moisture content after flooding was between 13 und 16 Vol.%. The salt content was 0 M.% (sample #14), 0.3 M.% (#16) and 0.9 M.% (#17). The samples were allowed to dry in ambient air over a period of 85 days. During that time, the samples were regularly weighed to determine their moisture content, and Radar measurements were performed across the samples. Directly underneath the samples, a steel bar of 12 mm diameter was located. Fig 8 (left) displays the measured Radar reflection coefficient, Fig. 8 (right) shows the real part of the dielectric permittivity which was calculated iteratively using Eqs (6) and (5). Both quantities are given as a function of the moisture of the three concrete cylinders with different salinity. For comparison, the calculated curves based on the analytical expressions for the complex dielectric permittivity of concrete at 2.45 GHz, as published by Schlemm [12], is also sketched in both figures.

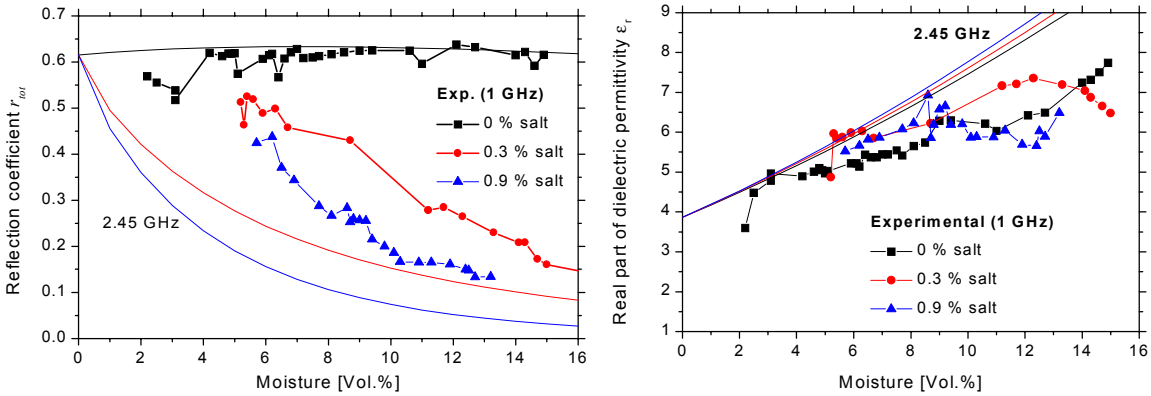

Fig. 8. Left: Measured Radar reflection coefficient of concrete cylinders with underlying steel bars, as a function of the moisture and salinity of the concrete. Right: Real part of the dielectric permittivity of the concrete, as deduced from the measured Radar transient time and reflection coefficient using Eqs. (6) and (5).

The qualitative agreement is surprisingly good. Considering that the published dielectric permittivity values are for 2.45 GHz, whereas our Radar measurement was conducted at 1 GHz, a deviation is to be expected. From our experimental data in Fig. 8, it becomes clear that the moisture and the salinity can be deduced independently from Radar measurements of the transient time and the reflection coefficient for a known depth of the steel reflector.

6. Measurements on highway bridges

Measurements on two German highway bridges (Uttrichshausen and Döllbachtal on Autobahn A7 near Fulda, see Fig. 9) were performed in order to test our Radar-Magnetic measurement vehicle and to verify the technique. On both bridge decks, the pavement was milled off so that the measurement could be performed directly on the concrete surface. On the Uttrichshausen bridge, two fields of 40 m and 80 m length were measured scanning three traces with 70 cm spacing in between. On the Döllbachtal bridge, one 90 m long field was measured in three traces directly on the concrete surface, another 50 m were measured through the pavement.

Fig. 9. Radar-Magnetic measurement on the Döllbachtal bridge.

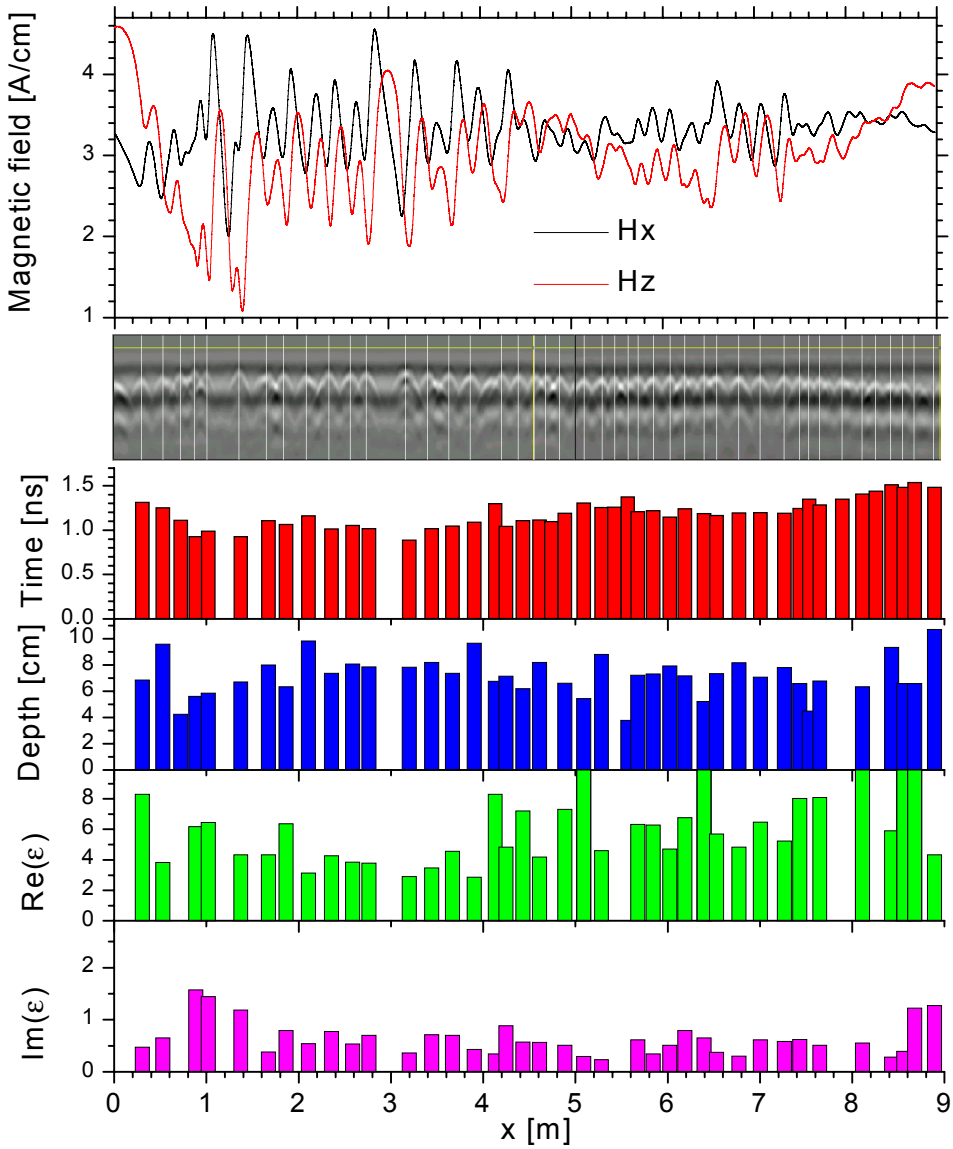

Fig. 10. Results of the Radar-Magnetic measurement on one 9 m-section of the Döllbachtalbrücke. The upper graph depicts the magnetic measurement and below the Radar B-scan. The vertical white lines mark the positions of the rebar found by our software for automated Radar analysis. The red columns indicate the measured transient time of the Radar pulse at the locations of the bars. The blue columns indicate the depths derived using Eq. (11) on the numerically differentiated magnetic field measurements. The green and magenta columns show real and imaginary part of the effective dielectric permittivity of the concrete, calculated from Eqs. (6) and (5).

The measurement vehicle operated reliably on the bridges. In most cases, Radar reflection positions agreed with the magnetic indications. As an example, the measured magnetic field and Radar data are depicted in Fig. 10 for one 9 m long section on the Döllbachtal bridge. The figure also shows the rebar locations identified by Radar, the corresponding transient time of the Radar pulse, the rebar depth as calculated from the magnetic data and the resultant components of the complex dielectric permittivity.

7. Conclusion and outlook

By combination of a Ground Penetrating Radar (GPR) reflection measurement with a static magnetic field measurement, a novel technique for non-destructive determination of moisture and salinity of concrete bridge decks has been developed which is based on determining the spatial distribution of the complex dielectric constant of the concrete.

A measurement vehicle, comprising a permanent magnet, four GMR magnetometers and a 1 GHz GPR head was developed and tested. Software for data analysis including automated peak detection was implemented for magnetic depth determination and Radar hyperbola identification. Measurements at concrete test blocks with defined chloride nests were performed. By relating the magnetically determined depth of the steel reinforcement bars in the upper layer to the reflection time measured by Radar, the effective dielectric permittivity of the intermediate concrete was determined. At the chloride nests, a significantly enhanced dielectric constant was determined. However, a large spread of experimentally found permittivity value was found. The error becomes larger for densely laid reinforcements. Consequently the precision is due to the limited precision of the magnetic depth determination because of the effects of neighbouring steels. As predicted by calculations, an analysis of the reflected radar amplitude yielded the imaginary part of the dielectric constant, also expressed as the loss tangent. It was verified with concrete samples of defined moisture and salinity that an independent determination of moisture and salinity is possible if the concrete is not too dry.

The Radar-Magnetic measurement system was tested on two German highway bridge decks. With a data acquisition speed of about 2 m/s, 200 m of bridge deck was examined in three parallel traces. The complex dielectric constant of the concrete close to the surface was mapped at these locations. Further investigations have to be carried out in order to improve the performance of the system on paved concrete.

Even at this stage, our simple vehicle-based Radar-Magnetic measurement allows a convenient and easy means for non-destructive estimation of moisture and salinity of the reinforced concrete of unpaved or paved bridge decks, identifying suspicious locations which should be examined. In addition, the location and the depth of all steel reinforcement bars perpendicular to the scanning path in the upper layer are obtained.

Acknowledgements

The authors thank Dr. Peter Haardt (BASt) for initiating the project and for fruitful discussion, Walter Wolf for his help with the measurements, Dieter Lomparski and Marko Banzet (FZJ) for constructing and assembling the measurement wagon, and Gerd Berthold and Hartmut Lähner (BASt) for their assistance in the manufacturing of the concrete blocks and during the measurements. The work was partially supported by the German Ministry of Traffic under supervision of the Bundesanstalt für Straßenwesen (BASt), Bergisch Gladbach, contract no. FE15.386/2003/HRB.

References

[1] P. Haardt, M. Krause, D. Streicher, H.-J. Krause, *Scanning NDT-Methods for the inspection of highway structures*, in: Bridge Maintenance, Safety, Management and Cost, in: Proceedings of the Second International Conference on Bridge Maintenance, Safety and Management (IABMAS'04), Eds.: E. Watanabe, D.M. Frangopol and T. Utsunomiya, Kyoto, October 18-22, 2004.

[2] G. Schickert, M. Krause, H. Wiggenhauser, *ZfPBau-Kompendium*, http://www.bam.de/service/publikationen/zfp_kompendium/welcome.html.

[3] Merkblatt für elektrochemische Potentialmessungen zur Ermittlung von Bewehrungsstahlkorrosion in Stahlbetonbauwerken (B3), Deutsche Gesellschaft für Zerstörungsfreie Prüfung e.V., Berlin (1990).

[4] W. Leschnik, *Feuchtemessung an Baustoffen – Zwischen Klassik und Moderne*, Feuchtetag '99, DGZfP-Berichtsband BB69-CD, Talk H2 (1999).

[5] C. Maierhofer, J. Wöstmann, *Investigation of dielectric properties of brick materials as a function of moisture and salt content using a microwave impulse technique at very high frequencies*, NDT&E International 31, 259-263 (1998).

[6] R. Springenschmid, *Anleitung zu Bestimmung des Chloridgehaltes von Beton*, Deutscher Ausschuß für Stahlbeton Heft 401; Hrsg: DAfStb, Berlin, pp. 7-44 (1989).

[7] C. Flohrer, *Messung der Betondeckung und Ortung der Bewehrung*, in: Fachtagung Bauwerksdiagnose, DGZfP-Berichtsband 66-CD, Talk 4 (1999).

[8] W. Ricken, G. Mehlhorn, W. Becker, *Determining of the concrete cover thickness and the bar diameter in reinforcing concrete with a method of eddy current testing*, Int. Symposium Non-destructive Testing in Civil Engineering (NDT-CE), Vol.1, pp. 197-204 (1995).

[9] R. Neumann und G. Dobmann, *Neue magnetische Gerätetechnik bei der Betondeckungsmessung,* in: Zerstörungsfreie Prüfung im Bauwesen, Ed.: G. Schickert, DGZfP, Berlin (1991).

[10] C. Maierhofer, S. Leipolt, J. Wöstmann, *Strukturuntersuchungen in Beton mit dem Impulsradar, in: Bauwerksdiagnose*, DGZfP-Berichtsband BB66-CD, pp. 47-57 (1999).

[11] H.-J. Krause, W. Wolf, W. Glaas, E. Zimmermann, M.I. Faley, G. Sawade, R. Mattheus, G. Neudert, U. Gampe, J. Krieger, *SQUID array for magnetic inspection of prestressed concrete bridges*, Physica C 368, 91-95 (2002).

[12] U. Schlemm, *Messung von Feuchte- und Salzprofilen mit Mikrowellen – Untersuchung von Störeinflüssen und Verbesserung der Messeigenschaften*, Dissertation, Techn. University Hamburg-Harburg (2003).